HHS Public Access

Author manuscript

Adv Mater. Author manuscript; available in PMC 2022 January 18.

Published in final edited form as:

Adv Mater. 2021 April ; 33(17): e2008553. doi:10.1002/adma.202008553.

Degradable and Removable Tough Adhesive Hydrogels

Benjamin R Freedman[1,2], **Oktay Uzun**[2], **Nadja M Maldonado Luna**[1,2,3], **Anna Rock**[2], **Charles Clifford**[1], **Emily Stoler**[2], **Gabrielle Östlund-Sholars**[2], **Christopher Johnson**[2], **David J Mooney**[1,2]

[1]John A. Paulson School of Engineering and Applied Sciences, Harvard University, Cambridge, MA, USA

[2]Wyss Institute for Biologically Inspired Engineering, Harvard University, Boston, MA, USA

[3]Department of Mechanical Engineering, University of Puerto Rico-Mayaguez, Puerto Rico, USA

Abstract

The development of tough adhesive hydrogels has enabled unprecedented adhesion to wet and moving tissue surfaces throughout the body but are typically composed of non-degradable components. Here, we develop a family of degradable tough adhesive hydrogels containing ~90% water by incorporating covalently networked degradable crosslinkers and hydrolyzable ionically crosslinked main chain polymers. Mechanical toughness, adhesion, and degradation of these new formulations was tested in both accelerated *in vitro* conditions and up to 16-weeks *in vivo*. These degradable tough adhesives were engineered with equivalent mechanical and adhesive properties to nondegradable tough adhesives, capable of achieving stretches > 20 times their initial length, fracture energies >6kJ/m^2, and adhesion energies >1000J/m^2. All degradable systems showed complete degradation within 2-weeks under accelerated aging conditions *in vitro* and weeks to months *in vivo* depending on the degradable crosslinker selected. Excellent biocompatibility was observed for all groups after 1, 2, 4, 8, and 16 weeks of implantation, with minimal fibrous encapsulation and no signs of organ toxicity. On-demand removal of the adhesive was achieved with treatment of chemical agents which did not cause damage to underlying skin tissue in mice. The broad versatility of this family of adhesives provides the foundation for numerous *in vivo* indications.

Keywords

hydrogel; adhesive; bioinspiration; degradation; biomaterial; animal study; slug

Corresponding Author: David J. Mooney, Ph.D., 319 Pierce Hal, Cambridge, MA 02138 USA, Phone: 617-384-9624, mooneyd@seas.harvard.edu.

Author Contributions: All authors contributed towards the production of this manuscript.

Competing Interests Statement

The authors receive grant support through the NIH and Wyss Institute. The views and opinions expressed in this article are those of the authors and do not necessarily reflect the position of the Wyss Institute for Biologically Inspired Engineering at Harvard University.

Introduction

Hydrogel-based biomaterials are broadly applied to treat injuries throughout the body because their water content is similar to that of native biological tissue and they have the potential for tissue reinforcement and therapeutic delivery.[1] However, most hydrogels have material toughness many hundreds of times less than that of native tissue,[2, 3] which limits their capacity to serve as tissue replacements and controlled drug release systems. To overcome this challenge, engineering hydrogels with high toughness has been explored.[4] One strategy to engineer high mechanical toughness within hydrogels is to utilize an interpenetrating network (IPN) of a physically crosslinked polymer network with a covalently crosslinked network (e.g., tough gels composed of alginate and polyacrylamide).[2] Their high toughness under loading is attributed to energy dissipation through dissociation of physical crosslinks, combined with distribution of applied stresses throughout the network due to inherent high elasticity of the covalent network.

The ability of these tough hydrogels to function as an adhesive (tough adhesive) to diverse tissue surfaces has recently been developed,[3, 5, 6] and they have the ability to adhere to wet (blood exposed) and dynamic surfaces with unprecedented adhesion energies. To generate the tough adhesive, the tough hydrogel is coated with a chitosan-based layer with the addition of coupling agents.[3] After application, the chitosan layer diffuses quickly into the tough hydrogel and adjacent tissue surface to form strong adhesion through a combination of electrostatic interactions, physical interpenetration, and covalent bonding. The tough hydrogel plays a critical role to dissipate energy at the adhesive interface and prevent cohesive failure of the matrix. However, the tough gels and adhesives are typically formulated using permanent non-degradable materials that remain in the body long-term or require a second procedure for removal after implantation. A tough adhesive with tunable degradation would enable expanded applications in biomedicine.

Biodegradation of hydrogels typically occurs through degradation of polymeric backbones or cleavage of its crosslinking chemical bonds and may be influenced by local mechanical loading, pH, and immune activity. In this study, biodegradable tough adhesive hydrogels were engineered with tunable mechanical properties, high-strength adhesion, and controlled degradation. The typical non-degradable tough adhesive was converted to a degradable tough adhesive by either replacement of the non-degradable acrylate-functionalized crosslinker (N,N'-methylenebis(acrylamide), MBAA) with hydrolytically or enzymatically degradable analogs, or introduction of a degradable alginate polymer[7, 8] (Figure 1a). The hydrolytically degradable crosslinkers selected were poly(ethylene glycol)-diacrylate (PEGDA), poloxamer diacrylate (PoloxDA), and oxidized alginate methacrylate (OxAlgMA) (Figure 1b), as the introduction of methacryloyl substituent groups enables the materials to be crosslinked on demand.[9] Degradation of PEGDA and PoloxDA crosslinkers within the tough hydrogels is possible through a hydrolytically cleavable ester bond. Degradation of GelMA is possible through digestion of gelatin with collagenase,[10] and degradation of HAMA is possible through digestion of hyaluronic acid with hyaluronidase. The mechanical and adhesive properties, as well as degradation *in vitro* and *in vivo*, of tough hydrogels synthesized with several degradable crosslinkers and polymers are demonstrated.

Given the properties of these adhesives, these materials may have a broad set of biomedical applications.

Results

Tough Hydrogels with Degradable Covalent Crosslinkers Maintain High Toughness and Adhesion

Hydrogels synthesized with the various crosslinkers were first optimized for high toughness by tuning the crosslinker concentration. Experiments first determined the optimal degradable covalent crosslinker concentration, starting from 0.06 (MBAA/acrylamide wt.%).[2] In short, previous work[2] established that this density optimization is critical to achieve peak fracture energies. High covalent crosslink densities result in shorter chains and low fracture energy due to dissipation of energy in the entire chain as each chain breaks. Low covalent crosslink densities result in high compliance and low alginate network unzipping to dissipate energy. As the degree of acrylate functionalization may vary between these crosslinkers, the concentration necessary to optimize gel mechanics also varied. The new crosslinkers were utilized at ratios ranging from 0.5 to 2-fold of that concentration to optimize hydrogel toughness, stretch, and maximum stress (Figure S1, S2). From these initial formulation studies, hydrogels were synthesized using the optimized concentration for each crosslinker. Tensile testing revealed that gels made with PEGDA, PoloxDA, and GelMA had material maximum stretch, maximum stress, and fracture toughness equivalent or even greater than gels crosslinked with the non-degradable MBAA (Figure 2a-d). Gels made with OxAlgMA and HAMA exhibited significantly lower mechanical properties. Evaluation of adhesive properties on wet porcine skin revealed that hydrogels formulated with PEGDA, PoloxDA, and GelMA had very high adhesion energies, similar to that of adhesives formed with MBAA (Figure 2e), while OxAlgMA and HAMA had significantly lower adhesion energies.

In Vitro Gel Degradation

The degradation kinetics of the various adhesives were next tested *in vitro*, under accelerated aging conditions. All tough hydrogels crosslinked with degradable crosslinkers exhibited a rapid, largely linear weight loss with time under these conditions, with all but the HAMA gels completed degraded by two weeks. In contrast, the MBAA gels exhibited no weight loss over this time, as expected (Figure 2f).

In parallel experiments, the incubation buffer was collected over time and evaluated for residual acrylamide release. A small quantity of AAM was rapidly released from the gels, regardless of crosslinker used, followed by no measurable further release (Figure S3).

Degradation and Biocompatibility In Vivo with Degradable Covalent Network

The degradation of tough hydrogels was next compared to non-degradable hydrogels over time in a subcutaneous implantation model in mice (Figure 3a). Degradation was evaluated by assessing changes in hydrogel thickness with high frequency ultrasound (HFUS) and quantifying the dry weights of explanted hydrogels (Figure 3b-e). PEGDA and PoloxDA crosslinked gels were largely degraded by 4-weeks post implantation, as indicated by both imaging and hydrogel dry weights following harvest. HAMA and OxAlgMA crosslinked

gels exhibited slower degradation profiles, with no significant changes observed in imaging but significant dry weight changes noted over 16-weeks. In contrast, GELMA crosslinked gels showed no evidence of degradation over this time when analyzed via imaging or dry weight analysis.

The biocompatibility of the various tough hydrogels was quantified by examining histological changes adjacent to the hydrogel and skin, and in liver, kidney, and spleen tissues. Scores for cell infiltration and capsule thickness were applied by a blinded histopathologist to differentiate among research groups. In all groups, minor fibrous encapsulation of gels was observed over time (Figure 4) with no signs of toxicity observed in the spleen, liver, or kidney (Figure S4-6). By 4-weeks, the PEGDA and PoloxDA gels degraded substantially, with small gel fragments present until 8-weeks. Among these faster degrading gels, the PoloxDA crosslinked gels led to elevated cell infiltration and a slightly larger capsule than the MBAA and PEGDA gels, although the capsule was overall minimal (Figure 4a-c). Among the more slowly degrading gels, HAMA gels had elevated cell infiltration and capsule grades, and had increased cell infiltration (Figure 4d-f).

Effect of degradable ionic interpenetrating network on tough adhesive mechanics and biodegradation

To test whether the slow degradation observed for OxAlgMA, GelMA, and HAMA crosslinkers could be accelerated, non-degradable alginate within the ionic network was replaced with oxidized alginate (Algoxalate, OxAlg) (Figure S7a). High maximum stretch and toughness were also observed for hydrogels containing oxidized alginate (Figure S7b,c). HAMA gels containing oxidized alginate showed increased degradation by 16-weeks post implantation, but this was not observed for OxAlgMA and GelMA crosslinked gels (Figure S7d). Similar to degradable tough gels not containing oxidized alginate, minor fibrous encapsulation of all gels was observed over time (Figure S7e) with no signs of toxicity observed in the spleen, liver, or kidney organs (Figure S8).

Addition of removal agents results in non-damaging detachment from skin surfaces

Although the tough adhesive generates extremely strong adhesion,[3] it may be useful or necessary to remove the adhesive on-demand for certain applications prior to its degradation. Therefore, the effect of different removal agents designed to target the tough hydrogel and chitosan adhesive surface was explored in the non-degradable system. It was first hypothesized that weakening of the energy dissipating features of the tough hydrogel could be a viable target to decrease material properties and adhesion, therefore tough hydrogels were treated with physiologically benign agents either designed to act as calcium chelators (citric acid, ethylenediaminetetraacetic acid (EDTA)), or to degrade alginate (hydrogen peroxide, alginate lyase) to weaken the ionic network (Figure 5a, Table S1).[11] Treatment with these various agents decreased the hydrogel mechanical properties over time, as expected (Figure 5b, S9). Additionally, chitosan degrades over time based on the degree of deacetylation of the chitosan,[12] which can be accelerated through treatment with lysozyme that acts on the glycoside bond subunits of chitosan.[13] Indeed, after treating chitosan with lysozyme (75mg/ml),[14] we observed a decrease in the molecular weight (Figure S10). The impact of these strategies on tough adhesive removal was next investigated. Peel adhesion

testing revealed that the adhesion energy significantly decreased following 10 min treatment with lysozyme, alginate lyase, and hydrogen peroxide (Figure 5c).

On-demand removal of the tough adhesive was next compared to removal of commercially available products, following adhesion to dry post-mortem mouse skin. Skin was examined both for residual adhesive and damage following removal, using histology and HFUS (Figure 5d). Tough adhesive removal following treatment with alginate lyase was qualitatively easier than without treatment, but no damage to the epidermis was observed in either situation. In contrast, current commercially available adhesives Dermabond™ and Loctite™ (cyanoacrylates) damaged the epidermis upon removal (Figure 5e).

Discussion

The biomedical translation of recently described tough adhesives[3] requires material degradation and removability for certain clinical indications. Here, we present strategies to engineer these features by incorporating hydrolytic and enzyme-mediated degradation mechanisms to degrade crosslinkers and polymers used to form tough adhesives. Degradable tough adhesives were synthesized with similar toughness and adhesion to the original formulation. Lead formulations were shown to degrade at varying rates both under accelerated aging conditions *in vitro* and in a subcutaneous implantation model *in vivo*. Overall, excellent biocompatibility was observed *in vivo*, with minor encapsulation. Removability of the adhesives was enhanced with the addition of agents that prompt alginate and chitosan degradation and allowed for negligible damage to the epidermis when removed from mouse skin, unlike removal of a commercial cyanoacrylate.

The physical properties achieved with several degradable tough hydrogel formats and adhesives are comparable to the previously described nondegradable tough hydrogels and tough adhesives[2, 3] and higher than other recently reported bioadhesives.[15] [16] Substitution of MBAA with PEGDA, PoloxDA, and GelMA resulted in the highest mechanical toughness and adhesion energies achieved. Although mechanical toughness was decreased in PoloxDA gels compared to MBAA gels, adhesion energy remained high, likely due to exceeding the upper limit in adhesive failure versus cohesive failure of the tough hydrogel.[3] The use of certain crosslinkers resulted in lower mechanical touchiness even though the polymer content remained constant in the different gel conditions. These differences in physical properties may be due to differences in the degree of acrylate substitution or the molecular weight of the linkers. Replacement of algoxalate into the alginate network decreased mechanical toughness of the tough gels, likely due to the decrease in alginate molecular weight during oxidation.[8] Taken together, these new formats allow tunability in mechanics and adhesion, which can enable broad applications of this material base.

The tunable versatility demonstrated in the degradation profiles ranging from weeks to months has not been reported previously. In accelerated aging conditions that contained the necessary hydrolytic and enzymatic environment to promote degradation, all gel conditions showed degradation within two weeks. Other strategies using *N,N'*-bis(acryloyl)cystamine degradable crosslinkers show rapid degradation and swelling over 48h *in vitro*, but did not

evaluate performance *in vivo*.[17] In the subcutaneous implantation model, the hydrolytic degradation environment is mimicked, enabling fast degradation of PEGDA and PoloxDA gels. PEGDA has previously been reported to exhibit excellent biocompatibility and is susceptible to degradation via hydrolysis of its end-group acrylate esters.[18] PoloxDA is a triblock copolymer that exhibits rheologic, anti-thrombotic, anti-inflammatory, and cytoprotective activities in various tissue injury models.[19] For OxAlgMA, GelMA, and HAMA crosslinkers, however, the subcutaneous environment led to overall slower degradation. Although OxAlgMA exploits the degradation of methacrylated oxidized alginates within the covalent network [8, 20], these gels experienced lower degradation, potentially due to the low degree of alginate oxidation in this polymer. Gelatin methacrylate (GelMA) was chosen based on the presence of matrix metalloproteinases (MMPs) following injury[21] that can degrade this material[22] However, these GelMA studies lacked injury at the implantation site which may have limited the degradation of these gels. Similarly, the natural abundance of hyaluronidase in the subcutaneous implant model is likely lower than that in anatomical locations involving joint lubrication, wound healing, and angiogenesis after enzymatic degradation.[23] The possible increase in weight of OxAlgMA and GelMA crosslinked gels may be due to cell infiltration and matrix secretion, or adherent surrounding tissue that was not possible to remove prior to sample dehydration. Although HAMA gels showed high cell infiltration, their overall degradation was slow. We speculate that this may be due to the molecular weight of HAMA used (10kDa). HA is degraded *in vivo* by two hyaluronidases, Hyal-1 and Hyal-2. Hyal-2 has greater specificity to higher molecular weight HA whereby larger fragments generated are ultimately internalized by cells and degraded to smaller tetrasaccharides by Hyal-1 within lysosomes and endosomes. [24] It is plausible that Hyal-2 mediated cleavage may contribute to degradation of HAMA crosslinked gels; therefore, future work will explore use of a higher molecular weight HAMA within the degradable tough adhesives.

Minor inflammation and capsule formation up to 16-weeks post implantation were found with the degradable adhesives in a mouse model. Histological scoring for cell infiltration and capsule formation was elevated in PoloxDA and HAMA gels compared to MBAA gels; however, this effect was small and does not indicate a potent immune response. Furthermore, the nondegradable gels prevented cell infiltration due to their nano porosity and tough mechanics, while the degradable gels exhibit weakening that likely allows for deformation and cell infiltration.

Studies have shown that the degradation of adhesives may cause an inflammatory response to surrounding tissues.[25, 26] This response was not observed in any of the lead formulations tested here. Findings with the tough gels contrast to reports from alkyl cyanoacrylates that produce cyanoacetate and formaldehyde during degradation, limiting their approval for topical use only (2-octyl cyanoacrylate, Dermabond).[25] Our degradable adhesive also avoids use of native proteins and glutaraldehyde, such as in BioGlue, which has induced potent inflammatory responses requiring surgical removal when used in certain indications. [27]

Another limitation during degradation of many adhesives is excessive swelling. For certain indications, swelling of Floseal (gelatin and thrombin) in vascular surgery caused epidural

spinal cord compression and neuro complications. [28] Similarly, DuraSeal (PEG ester and trilysine amine solutions) swelling has resulted in spinal cord compression[29] and Surgicel (oxidized cellulose) swelling has prompted its immediate removal just 1-day after surgery. [30] Longitudinal ultrasound imaging revealed minor additional swelling of degradable tough adhesives following implantation. If swelling were found to be concern with the tough adhesives in the future, incorporation of poly(N-isopropylacrylamide) (PNIPAm) can eliminate swelling of this type of gel.[5]

A potential concern with these tough hydrogels is that residual acrylamide monomer or PAAm may be released over time, and acrylamide can be neurotoxic at high concentrations. [31] The total amount of unreacted monomer after initial washes was similar to published thresholds,[32] suggesting that extensive washing during fabrication can allow the residual acrylamide to be lowered to safe levels and could be further improved if necessary. PAAm is present in a wide variety of water treatment products, food products, cosmetics, and personal care products.[33] The Food and Drug Administration (FDA) allows PAAm (with less than 0.2% acrylamide monomer) to be used as a film former in the imprinting of soft-shell gelatin capsules[34] and as a denture adhesive.[35] Residual acrylamide monomer is likely an impurity in most PAAm preparations, ranging up to 0.1%.[32] Higher levels of acrylamide monomers are present in solid formulations, as PAAm is used in more than hundred cosmetic formulations at concentrations up to 20%.[36] Unlike its monomer, PAAm itself is not significantly toxic; an acute oral toxicity study of PAAm in rats reported that a single maximum oral dose of 4.0 g/kg body weight was tolerated.[36]

More broadly, the components of the tough adhesives are currently approved for use by the FDA in other products. Alginate, chitosan, and polyacrylamide are used in commercial grade products for both internal and external uses.[3, 5, 37] Alginate has been used in many wound dressings (e.g., Algicell® (Derma Sciences)) as has chitosan (e.g., ChitoFlex (Tricol Biomedical)). Likewise, polyacrylamide is approved for use as a filler material in urinary incontinence (Bulkamid®).[38] The spectrum of degradable profiles in our materials spans that of typical degradation profiles for COSEAL (30 days),[39] Floseal (28-56days), [40] Duraseal (56 days),[41] and TISSEEL (10-14 days).[42] This tunability, in addition to strong adhesion biocompatibility and stretchability, may enable broad applications based on indication and disease state.

This study demonstrated that standard, commercially available reagents can weaken the tough hydrogel or bridging polymer surfaces on demand, and reduce the energy required for their removal. Removal of the tough adhesive did not cause noticeable damage to underlying tissue, as analyzed via histology. Administration of alginate lyase and lysozyme led to the most dramatic weakening of the tough adhesive. Surprisingly, while strategies to chelate calcium from the gels decreased material toughness, adhesion was still maintained. These findings suggest a key role of even the uncross-linked alginate network in supporting adhesion, perhaps through the covalent coupling to chitosan. While the tough adhesive provides a window of time for anatomical location optimization, the ability to detach may be important for scenarios of incorrect placement or removal after tissue healing is complete. Triggerable detachment may also enable these adhesives to be used in minimally invasive

surgical procedures whereby the adhesive functions to aid in surgical access to a diseased organ.

In conclusion, we engineered a family of biodegradable tough adhesive materials to expand the utility of tough adhesive hydrogels for indications in the medical field requiring material degradation. For indications requiring high mechanical toughness and adhesion, these formats can provide degradation kinetics ranging from approximately 2 weeks to several months *in vivo*. In cases where lower mechanical toughness and adhesion may be desired, degradation profiles scale on the order of months *in vivo*. This broad versatility provides the foundation for future studies to evaluate performance of these formulations in additional *in vivo* indications.

Methods

Oxidized Alginate Synthesis

Oxidized alginate was prepared by a two-step process. First, 5% of the alginate's alcohols were converted to aldehyde via sodium periodate to create hydrolytic acetal groups on the alginate chains[8, 43] followed by a second oxidation of aldehydes to carboxylic acids using sodium chlorite to improve biocompatibility. Briefly, a 1% w/v solution of alginate (Dupont, ProNova, UP MVG, #4200101) was prepared. For 1g of alginate, 60.7mg of sodium periodate (Sigma-Aldrich, 311448) was added to the solution (sodium periodate added at a molar equivalent to the percent moles of monomer to be oxidized in the alginate), which was left to react overnight while stirring protected from light. 1.8g of sodium chloride was next added to prepare a 0.3 M solution and the oxidized product was purified by Tangential Flow Filtration (TFF) with a 1 kDa MWCO hollow fiber columns (Spectrum Labs) using progressively decreasing salt solution washes from 0.15 M NaCl to pure water in 0.05 M decreasing increments. The purified solution was then frozen overnight at −80C and lyophilized. Once dried, the aldehyde-converted alginate was prepared in water and an aliquot of DMSO (VWR, BDH1115) was added (5 molar equivalent to the expected moles of aldehydes in the alginate) followed by 102.7mg of sodium chlorite (VWR, 97066-116, 2M equivalence to aldehydes). The reaction was left to stir overnight at room temperature (RT). The next day, sodium chloride was added to the solution to reach 0.3 M and the oxidized product was again purified by TFF. The purified final product solution was frozen at −80C overnight and lyophilized.

Oxidized Alginate Methacrylate Synthesis

Methacrylated oxidized-alginate was prepared by reacting 200mg of alginate (2.5% oxidized) (MVG, NovaMatrix, Norway) with 2-Aminoethylmethacrylamide hydrochloride-AEME (Sigma, 900652). 2.5% oxidized sodium alginate was dissolved in a 10mL buffer solution [0.75% (wt/vol), pH ~6.5] of 100 mM MES. The coupling reagents were added to activate the carboxylic acid groups of alginate (130mg N-hydroxysuccinimide (NHS, Thermofisher) and 280mg 1-ethyl-3-(3-dimethylaminopropyl) carbodiimide hydrochloride (EDC, Sigma)). After 5 min, AEMA (224 mg; molar ratio of NHS:EDC:AEMA = 1:1.3:1.1) was added to the product and the solution was stirred at RT for 24 h. The mixture was precipitated in acetone, filtered, and dried in a vacuum overnight at RT.

Gelatin Methacrylate Synthesis

For *in vivo* procedures, gelatin methacrylate (GelMA) was purchased (Sigma, 900496). For *in vitro* procedures, GelMA was synthesized by dissolving Type A porcine skin gelatin (Sigma, G1890) at 10% (w/v) in 1x Dulbecco's phosphate buffered saline without calcium at 50C for 1 h. Then, methacrylic anhydride (Sigma) was added dropwise to a final volume ratio of 1:4 methacrylic anhydride:gelatin solution. This resulted in GelMA with a degree of substitution of 80%. The solution was stirred at 50 C for 1 h, and then diluted 5X with DPBS. The resulting mixture was dialyzed for 3-4 d against distilled water with frequent water replacement in 12-14 kDa molecular weight cutoff tubing (Spectrum Labs). The dialyzed solution was lyophilized, and the resulting GelMA was stored at −20 C freezer until use.

Tough Gel Synthesis

Tough gels were synthesized by mixing one syringe containing a 10mL solution of 2.2% sodium alginate [combining a high (MW=200kDa) and low (MW=30kDa) molecular weight alginate at 1:1 ratio; MVG or LF20/40 and VLVG or LF 20/40 irradiated, (Pronova, Novamatrix Norway)] and 13.5% acrylamide (Sigma, A8887) in HBSS (Gibco), 36µl of 2% N,N'-methylenebis(acrylamide) (Sigma, M7279), and 8µl of TEMED (Sigma, T7024), with a second syringe containing 226µl of 6.6% ammonium persulfate (Sigma, A9164), and 191µl of 0.75M calcium sulfate dihydrate (Sigma, 31221). The gel was cast into molds ($80x15x1.5mm^3$) sealed on both sides with glass and left to crosslink for 24h. After 24h, tough gel strips were removed from molds and stored in sealed plastic bags at 4°C.

For degradable tough gels, the degradable crosslinker was first mixed with alginate-pAAM stock solutions. For PEGDA (Mn: 250Da, Sigma, 475629) crosslinked gels, 30 µL of a stock solution (100 mg of PEGDA in 1mL of HBSS buffer) was mixed with 10 mL of the alginate-pAAM monomer mixture prior to syringe mixing with calcium sulfate dihydrate, TEMED, and ammonium persulfate. For the remaining cross linkers (GelMA, PoloxDA (PolySciTech, Poloxamer 407, AI146, Mw: 12.5kDa), OxAlgMA, and HAMA (Creative PEG Works, HA-301, Mn: 10kDa)), 16 mg of the cross linker powder was added into 10 mL of the monomer mixture and vortexed for approximately 30 min until a homogenous mixture was achieved.

Hydrogel Mechanical Properties

Pure shear tests were carried out to measure the matrix toughness. In brief, rectangular specimens ($20x5x1.5\ mm^3$) were tested in tension (Instron 3342, 10N load cell) at 100mm/min. From the stress-stretch curves, the matrix maximum stretch, maximum stress, and fracture energy were calculated [2] using custom MATLAB code.

Adhesive Application and Adhesion Energy Measurement

Ultrapure chitosan (2%) (54046, Heppe Medical Chitosan, Halle, Germany) and coupling reagents (1-ethyl-3-(3-dimethylaminopropyl) carbodiimide (Sigma E6383) and sulfated N-hydroxy-succinimide) (Thermofisher, PG82071) (12 mg/mL) were quickly mixed by vortexing. This mixture was applied to the surface of the tough gel ($25µL/cm^2$) and compressed to the skin surface.

Adhesion energy was measured with 180° peeling tests (Instron 3342) under uniaxial tension (100mm/min). The adhesion energy was measured with 180-degree peeling tests. A ribbon of the tough adhesive (15x1.5x80 mm3) was adhered to a substrate with one end open, forming a bilayer with an edge crack. The back of TA was also bonded to a rigid polyethylene terephthalate (PET) film with cyanoacrylate (Krazy Glue), in order to limit deformation to the crack tip, and thus all the work done by the machine would be equal to the energy dissipated at the crack tip. The free ends of TA and the substrate were attached to acrylic pieces, to which the machine grips were attached. A mechanical testing system (Instron 3342, 50N load cell) was used to apply unidirectional tension, while recording the force and the extension. The loading rate was kept constant at 100 mm/min. The adhesion energy was two times the plateau value of the ratio of the force and width.[3]

In Vitro Degradation Evaluation

For accelerated hydrolytic degradation, we combined 25U/mL collagenase and 25U/mL hyaluronidase in 1xPBS containing 1.5mM calcium. During accelerated degradation experiments, tough hydrogel disks (diameter = 6mm, thickness = 1.5mm) were submerged in buffer maintained at 37C and replaced daily. After set time points, hydrogel samples were collected, rinsed briefly in water, frozen at −20C, and lyophilized for one week, before dry weight measurement.

Characterization of the residual AAm monomer

Three circular gels (1.5mm thick, 3mm diameter) per time point were placed in a 24 well plate with 2 mL 1X PBS media to extract the residual monomer from the gels. Samples were aliquot and analyzed after 30min, 1 h, 1 d, 2 d and 6 d. A standard curve of acrylamide monomer (Sigma) in 1X PBS was prepared by serial dilutions and run on 0.1% formic acid as the mobile phase. An Agilent 1200-series high-performance liquid chromatography (HPLC) coupled with a mass spectrometer was used for detection.[44] Between runs, the machine was flushed, and the conditioned PBS was run to compare the integrated peak area in the total ion count channel of the sample to those of the known concentrations from the standard curve.

Subcutaneous Injury Model

All mouse experiments were conducted according to approved IACUC protocols. Balb/C mice at 6-8 weeks of age had tough hydrogels implanted subcutaneous. Briefly, animals were anesthetized with isoflurane (2-2.5%) and given buprenorphine subcutaneously (0.5mg/kg) for pain management. Hair on the mouse dorsum was removed with clippers and depilatory cream prior to adding three separate washes of betadine and ethanol. Animals were then transferred to the sterile field and placed beneath a separate sterile fenestrated drape. A small 6mm incision was made through skin in the animal’s back perpendicular to the midline, and then a pocket was created using scissors. Four separate gels (D=3mm, th=1.5mm) were then implanted subcutaneously, and the skin was closed with 4-0 Vicryl suture. Animals were monitored daily and evaluated for subsequent assays.

High Frequency Ultrasound Imaging (HFUS)

HFUS (VisualSonics Vevo 770 and Vevo 3100; 35-50MHz) was used to evaluate gel swelling and degradation in vivo. Axial images (30-40um resolution) were acquired that captured the skin and hydrogel. Images were quantified for the thickness of the hydrogel and surrounding capsule. For tough gels crosslinked with MBAA, PEGDA, and PoloxDA, imaging was completed after 1, 2, 4, and 8 weeks post implantation. For tough gels cross linked with MBAA, GelMA, HAMA, and OxAlgMA, imaging was completed after 4, 8, and 16 weeks. Images were analyzed for hydrogel thickness using ImageJ (NIH).

Tissue Collection

Mice were sacrificed at time points of interest to collect organs determined to be most sensitive to potential cytotoxic effects as well as implanted hydrogels. After euthanasia by CO_2 inhalation, blood was immediately collected via cardiocentesis in a small tube, centrifuged at 290 rcf for 10 minutes, and then the resulting serum was transferred to a new tube for storage at −80°C until analysis. After ultrasound imaging, an incision at the base of the skull was made to create subcutaneous space such that the skin and gels could be removed as the incision was extended on the periphery of the back. The gel diameter attached to the skin sample was measured and the implant site containing one gel was removed using an 8mm biopsy punch to be fixed alongside the collection of the other organs. To evaluate the degradation and/or swelling in vivo, the remaining gels were rinsed in HBSS, dehydrated, and weighed. Collected organs (kidneys, liver, spleen, skin surrounding the implant site) were placed in histological cassettes and then submerged in 4% paraformaldehyde (PFA) fixative at 4°C for 24hours. Organs were then washed in 1xPBS two times for 10 minutes, before brief storage in 70% EtOH at 4°C.

Histology

Samples were embedded in paraffin, sectioned, mounted, and stained with hematoxylin and eosin (H&E) by the Rodent Histopathology Core at Harvard Medical School (Boston, MA). Subsequently, all H&E stained slides were imaged on a ZEISS Axio Scan.Z1 high throughput slide scanner using ZEN (Version 3.0) software for acquisition and visualization. Images were captured at 10X objective on a bright field and captured with ZENBLUE 3.0 software. Images were then examined for inflammation, fibrotic response, and other pathologies by a blinded rodent histopathologist. Severity scores of 0-5 were assigned using blinded analysis of randomized samples. For each histologic aspect evaluated, a score of 0 indicated no change was observed, 1 indicated a trace amount was noted, 2 indicated mild, 3 indicated moderate, 4 indicated marked and 5 indicated severe. These scores served as discrete numerical bins for research comparison and were not intended to indicate overall clinical condition or outcome.

Gas Permeation Chromatography (GPC) of Chitosan Degradation with Lysozyme Treatment

Chitosan (3mg/mL) (Product#: 54046, 90% deacetylation, HMC, Germany) solutions were analyzed for their molecular weight after incubation with varying concentrations of lysozyme (L6876, Sigma) [17, 37, 75 mg/mL] for over time (1min, 10min, 30min, 100min).

Gas Permeation Chromatography (GPC) analysis was performed with Viscotek TDAmax equipped with a GPCmax solvent and sample delivery module, a TDA 305 triple detector, a UV detector 2600, a solvent saver device, and OmniSec software. The GPC column was single G4000PWxl (Tosoh Bioscience) with flow rate 0.75mL/min mobile phase- 0.1M sodium nitrate ($NaNO_3$), 0.01M monosodium phosphate NaH_2PO_4 and 0.075% sodium azide (NaN_3), buffered to pH 3.0 with phosphoric acid. The 100uL sample was filtered three times through 0.1μm PES. We monitored the change in weight average (Mw) and number average (Mn) molecular weight of the chitosan. The highest concentration of lysozyme (75mg/mL) resulted in the highest decrease in weight average molecular weight from 280kD to 178kD. Next, we increased the lysozyme concentration from 75mg/mL to 150mg/mL; we observed that the Mw decrease were similar between these two samples with 112kD. Of all conditions, the 75mg/mL lysozyme concentration performed best overall for chitosan degradation. We confirmed a similar lysozyme degradation profile using a different chitosan with a lower degree of deacetylation percentage (HMC-54039, 85% deacetylation).

Treatment with Removal Agents

Tough hydrogels were treated with several removal agents (alginate lyase, EDTA, citric acid, H_2O_2, lysozyme) for 1, 10, and 100 min. These agents were specifically chosen to weaken the toughness of the hydrogel, which is essential to generating tough adhesion. Calcium chelators (EDTA, citric acid, H_2O_2), alginate lyase, and lysozyme (degrades chitosan) were selected. Following treatment, tough hydrogel mechanical properties and adhesion energy were assessed. We evaluated adhesion energy for agents targeting both calcium chelation and alginate molecular weight that achieved the largest decrease in tough hydrogel toughness following treatment (EDTA, H_2O_2, alginate lyase), as well as lysozyme (chitosan). The ability for the materials to be removed without causing residual skin damage was examined in a subset of agents. Tough hydrogels, cyanoacrylate (Loctite 4541), and Dermabond® were adhered to the backs of freshly euthanized mice for 10 min prior to removal. The TA was treated with and without alginate lyase (n=4/group) as a proof of principal experiment, as this treatment performed the best in bench testing. The remaining groups did not receive removal agents. Following adhesive removal, skin samples were imaged using high frequency ultrasound to examine for any residual adhesive. Skin biopsies were then harvested, fixed in 4% PFA, washed in ethanol, embedded in paraffin, sectioned (5μm), stained (H&E), and imaged (Axio Scan, Zeiss).

Statistical Analysis

Data normality was assessed with Shapiro Wilk tests (SPSS). One-way (time) or two-way (healing and TA implantation) ANOVAs with post hoc Student’s t-tests were used. For non-parametric data, Scheirer-Ray-Hare test (nonparametric 2-way ANOVA) with Dunn’s tests for multiple comparisons were used.

Supplementary Material

Refer to Web version on PubMed Central for supplementary material.

Acknowledgments

This work was supported by the Wyss Institute for Biologically Inspired Engineering at Harvard and the National Institute on Aging of the NIH (F32AG057135, K99AG065495). We thank Michael Lewandowski for discussion.

References

[1]. Freedman BR, Mooney DJ, Adv Mater 2019, 31, e1806695. [PubMed: 30908806]

[2]. Sun JY, Zhao X, Illeperuma WR, Chaudhuri O, Oh KH, Mooney DJ, Vlassak JJ, Suo Z, Nature 2012, 489, 133. [PubMed: 22955625]

[3]. Li J, Celiz AD, Yang J, Yang Q, Wamala I, Whyte W, Seo BR, Vasilyev NV, Vlassak JJ, Suo Z, Mooney DJ, Science 2017, 357, 378. [PubMed: 28751604]

[4]. Zhao X, Soft Matter 2014, 10, 672. [PubMed: 24834901]

[5]. Blacklow SO, Li J, Freedman BR, Zeidi M, Chen C, Mooney DJ, Sci Adv 2019, 5, eaaw3963. [PubMed: 31355332]

[6]. Lazow SP, Labuz DF, Freedman BR, Rock A, Zurakowski D, Mooney DJ, Fauza DO, J Pediatr Surg 2020.

[7]. Lueckgen A, Garske DS, Ellinghaus A, Desai RM, Stafford AG, Mooney DJ, Duda GN, Cipitria A, Biomaterials 2018, 181, 189. [PubMed: 30086448]

[8]. Bouhadir KH, Lee KY, Alsberg E, Damm KL, Anderson KW, Mooney DJ, Biotechnol Prog 2001, 17, 945. [PubMed: 11587588]

[9]. Yue K, Trujillo-de Santiago G, Alvarez MM, Tamayol A, Annabi N, Khademhosseini A, Biomaterials 2015, 73, 254; [PubMed: 26414409] Van Den Bulcke AI, Bogdanov B, De Rooze N, Schacht EH, Cornelissen M, Berghmans H, Biomacromolecules 2000, 1, 31. [PubMed: 11709840]

[10]. Koshy ST, Ferrante TC, Lewin SA, Mooney DJ, Biomaterials 2014, 35, 2477. [PubMed: 24345735]

[11]. Li X, Xu A, Xie H, Yu W, Xie W, Ma X, Carbohydrate Polymers 2010, 79, 660.

[12]. Chenite A, Chaput C, Wang D, Combes C, Buschmann MD, Hoemann CD, Leroux JC, Atkinson BL, Binette F, Selmani A, Biomaterials 2000, 21, 2155. [PubMed: 10985488]

[13]. Loncarevic A, Ivankovic M, Rogina A, Journal of Tissue Repair and Regeneration 2017, 1.

[14]. Boryniec S, Strobin G, Struszczyk H, Niekraszewicz A, Kucharska M, International Journal of Polymer Analysis and Characterization 1997, 3, 9;Altinisik A, Yurdakoc K, J Appl Polym Sci 2011, 122, 7.

[15]. Yuk H, Varela CE, Nabzdyk CS, Mao X, Padera RF, Roche ET, Zhao X, Nature 2019, 575, 169. [PubMed: 31666696]

[16]. Chen J, Wang D, Wang LH, Liu W, Chiu A, Shariati K, Liu Q, Wang X, Zhong Z, Webb J, Schwartz RE, Bouklas N, Ma M, Adv Mater 2020, 32, e2001628. [PubMed: 32945035]

[17]. Yang H, Li C, Tang J, Suo Z, ACS Appl. Bio Mater 2019, 2, 5.

[18]. Browning MB, Cereceres SN, Luong PT, Cosgriff-Hernandez EM, J Biomed Mater Res A 2014, 102, 4244. [PubMed: 24464985]

[19]. Hunter RL, Luo AZ, Zhang R, Kozar RA, Moore FA, Ann Clin Lab Sci 2010, 40, 115; [PubMed: 20421622] Moloughney JG, Weisleder N, Recent Pat Biotechnol 2012, 6, 200. [PubMed: 23092436]

[20]. Shih TY, Blacklow SO, Li AW, Freedman BR, Bencherif S, Koshy ST, Darnell MC, Mooney DJ, Adv Healthc Mater 2018, 7, e1701469. [PubMed: 29441705]

[21]. Nagase H, Visse R, Murphy G, Cardiovasc Res 2006, 69, 562; [PubMed: 16405877] Csoka AB, Frost GI, Stern R, Matrix Biol 2001, 20, 499. [PubMed: 11731267]

[22]. Van den Steen PE, Dubois B, Nelissen I, Rudd PM, Dwek RA, Opdenakker G, Crit Rev Biochem Mol Biol 2002, 37, 375. [PubMed: 12540195]

[23]. Leach JB, Bivens KA, Patrick CW, Schmidt CE, Biotechnol Bioeng 2003, 11;Chen WY, Abatangelo G, Wound Repair Regen 1999, 7, 79; [PubMed: 10231509] Burdick JA, Chung C, Jia X, Randolph MA, Langer R, Biomacromolecules 2005, 6, 386; [PubMed: 15638543] Toole BP, J

Intern Med 1997, 242, 35; [PubMed: 9260564] Yang B, Zhang L, Turley EA, J Biol Chem 1993, 268, 8617; [PubMed: 7682552] Entwistle J, Hall CL, Turley EA, J Cell Biochem 1996, 61, 569; [PubMed: 8806080] Peach RJ, Hollenbaugh D, Stamenkovic I, Aruffo A, J Cell Biol 1993, 122, 257; [PubMed: 8314845] Bencherif SA, Srinivasan A, Horkay F, Hollinger JO, Matyjaszewski K, Washburn NR, Biomaterials 2008, 29, 1739. [PubMed: 18234331]

[24]. Harada H, Takahashi M, J Biol Chem 2007, 282, 5597. [PubMed: 17170110]

[25]. Taboada GM, Yang K, Pereira MJN, Liu SS, Hu Y, Karp JM, Artzi N, Lee Y, Nature Reviews Materials 2020.

[26]. Murdock MH, Chang JT, Luketich SK, Pedersen D, Hussey GS, D'Amore A, Badylak SF, J Thorac Cardiovasc Surg 2019, 157, 176. [PubMed: 30274840]

[27]. Ngaage DL, Edwards WD, Bell MR, Sundt TM, J Thorac Cardiovasc Surg 2005, 129, 937; [PubMed: 15821668] Pasic M, Unbehaun A, Drews T, Hetzer R, Interact Cardiovasc Thorac Surg 2011, 13, 532. [PubMed: 21807815]

[28]. Buchowski JM, Bridwell KH, Lenke LG, Good CR, Spine (Phila Pa 1976) 2009, 34, E473. [PubMed: 19478651]

[29]. Lee SH, Park CW, Lee SG, Kim WK, Korean J Spine 2013, 10, 44. [PubMed: 24757459]

[30]. Menovsky T, Plazier M, Rasschaert R, Maas AI, Parizel PM, Verbeke S, Minim Invasive Neurosurg 2011, 54, 257. [PubMed: 22278791]

[31]. Pennisi M, Malaguarnera G, Puglisi V, Vinciguerra L, Vacante M, Malaguarnera M, Int J Environ Res Public Health 2013, 10, 3843. [PubMed: 23985770]

[32]. Int J Toxicol 2005, 24 Suppl 2, 21. [PubMed: 16154914]

[33]. Guezennec AG, Michel C, Bru K, Touze S, Desroche N, Mnif I, Motelica-Heino M, Environ Sci Pollut Res Int 2015, 22, 6390. [PubMed: 25253053]

[34]. Sec. 172.255 Polyacrylamide, 2019, FDA, CFR 21, https://www.accessdata.fda.gov/scripts/cdrh/cfdocs/cfcfr/CFRSearch.cfm?fr=172.255&SearchTerm=polyacrylamide

[35]. Sec. 872.3480 Polyacrylamide polymer (modified cationic) denture adhesive., 2019, FDA, Subpart D--Prosthetic Devices, CFR-21, https://www.accessdata.fda.gov/scripts/cdrh/cfdocs/cfcfr/CFRSearch.cfm?fr=872.3480

[36]. Deckner GE, 1993. LOW pH AQUEOUS COSMETIC GEL CONTAINING NON-IONIC POLYACRYLAMIDE DERIVATIVES, 1445, Patent, WIPO (PCT), WO, WO1993007856A1,

[37]. Darnell MC, Sun JY, Mehta M, Johnson C, Arany PR, Suo Z, Mooney DJ, Biomaterials 2013, 34, 8042. [PubMed: 23896005]

[38]. Lose G, Mouritsen L, Nielsen JB, BJU Int 2006, 98, 100; [PubMed: 16831152] Kasi AD, Pergialiotis V, Perrea DN, Khunda A, Doumouchtsis SK, Int Urogynecol J 2016, 27, 367. [PubMed: 26209952]

[39]. FDA, 2003, Summary of Safety and Effectiveness Data, PMA: P030039, 1475, Report, https://www.accessdata.fda.gov/cdrh_docs/pdf3/P030039b.pdf

[40]. FDA, 1999, Summary of Safety and Effectiveness. PMA: P990009, 1476, Report, https://www.accessdata.fda.gov/cdrh_docs/pdf/P990009B.pdf

[41]. FDA, 2009, Summary of Safety and Effectiveness Data. PMA: P080013, 1477, Report, https://www.accessdata.fda.gov/cdrh_docs/pdf8/P080013b.pdf

[42]. FDA, 1998, Highlights of Prescribing Information: TISSEEL, 1478, Report, https://www.fda.gov/media/71674/download

[43]. Boontheekul T, Kong HJ, Mooney DJ, Biomaterials 2005, 26, 2455. [PubMed: 15585248]

[44]. Al-Taher F, 2012, Analysis of acrylamide in french fries using Agilent Bond Elut QuEChERS AOAC kit and LC/MS/MS, 1469, Report, https://www.agilent.com/cs/library/applications/5990-5940EN.pdf

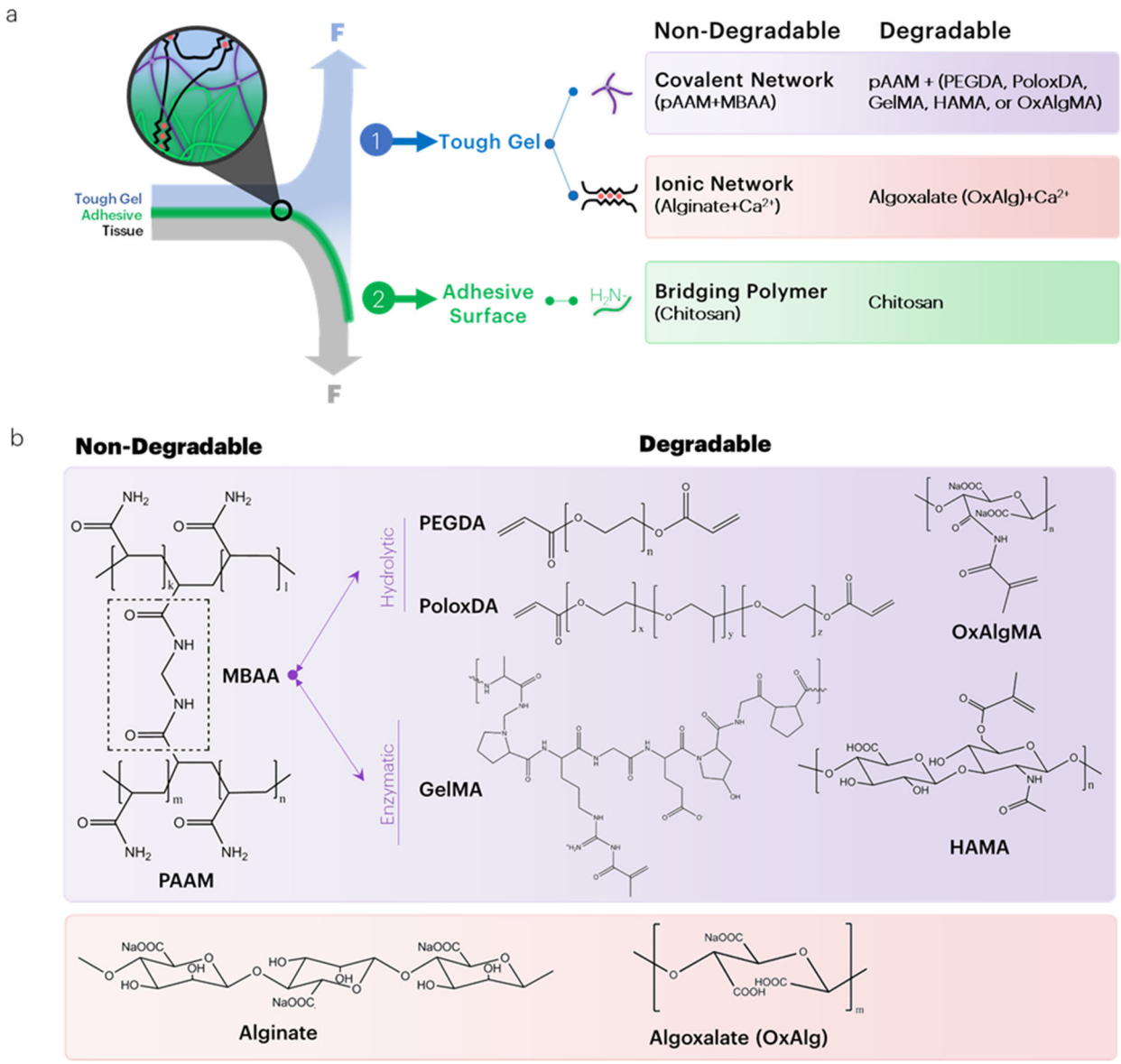

Figure 1: Overview of strategies to engineer degradable tough adhesives.

(**a**) Several strategies were explored to engineer degradable tough adhesives. To make the covalent network degrade, the non-degradable crosslinker of polyacrylamide is replaced with acrylate-functionalized degradable linkers. To make the ionic network degradable, oxidized alginate (algoxalate) was used. Chitosan degradation occurs under physiological conditions based on the degree of deacetylation of chitin. (**b**) For hydrolytically degrading tough gels, MBAA is replaced with either PEGDA, PoloxDA, or OxAlgMA. For enzymatically degrading hydrogels, MBAA is replaced with either GelMA or HAMA. Within the ionic network, alginate is replaced with its oxidized analog, algoxalate.

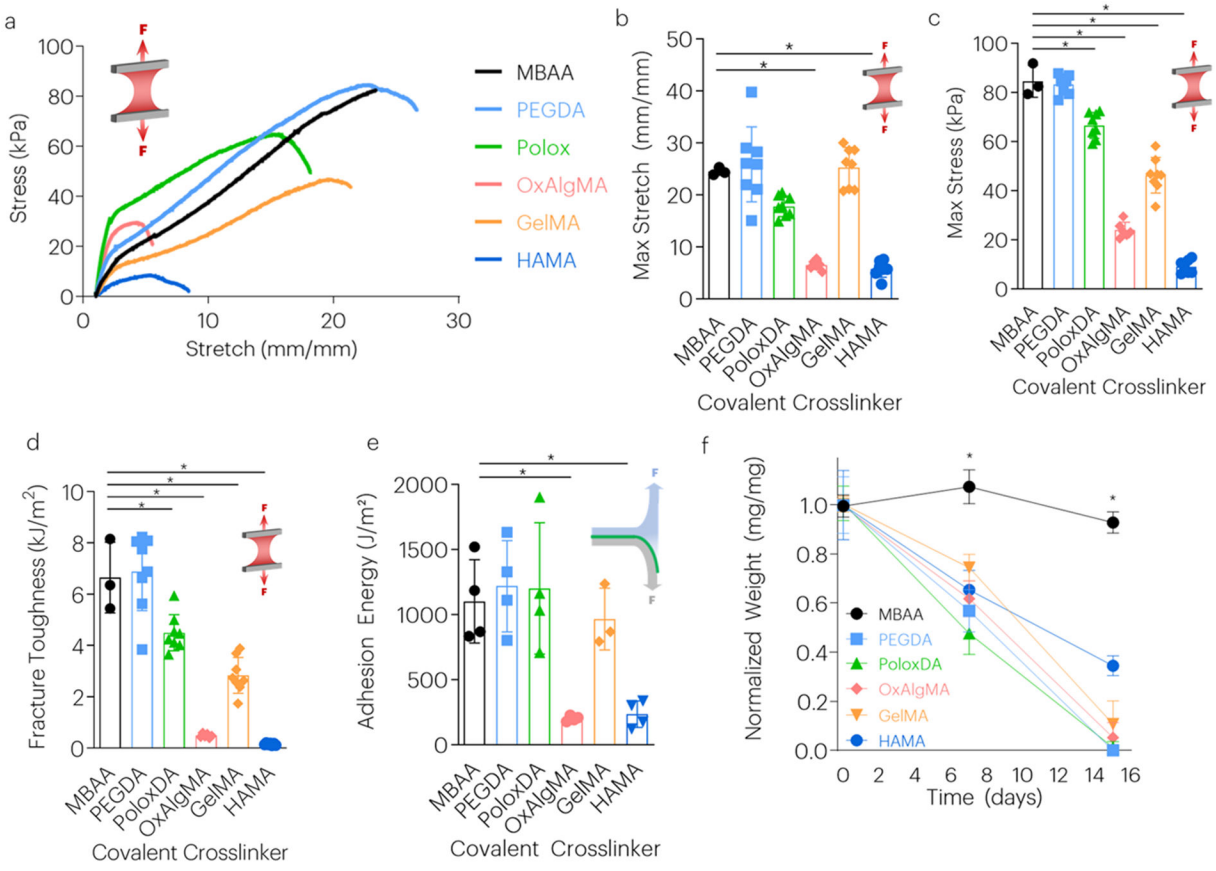

Figure 2: Tough Hydrogels with Degradable Covalent Network Maintain High Toughness and Adhesion.

(**a-d**) The effect of different covalent crosslinkers on maximum stretch, stress, and fracture toughness. The covalent crosslinkers tested with associated concentrations *(crosslinker/ acrylamide wt.%)* were: MBAA (0.06), PEGDA (0.06), PoloxDA (0.12), OxAlgMA (0.12), GelMA (0.03), and HAMA (0.06). **P*<0.01 between time points. Mean values are shown and error bars represent ± s.d. (n=3-8 samples/group), as analyzed by a one-way ANOVA with post hoc t-tests with Bonferroni correction. (**e**) The effect of covalent crosslinker on adhesion energy. **P*<0.01 between groups. Mean values are shown and error bars represent ± s.d. (n=3-4 samples/group), as analyzed by a one-way ANOVA with post hoc t-tests with Bonferroni correction. (**f**) The effect of crosslinker type on TA dry weight over time was evaluated with exposure to accelerated aging buffer. **P*<0.01 between time points. Mean values are shown and error bars represent ± s.d. (n=3-4 samples/group), as analyzed by a one-way ANOVA with post hoc t-tests with Bonferroni correction.

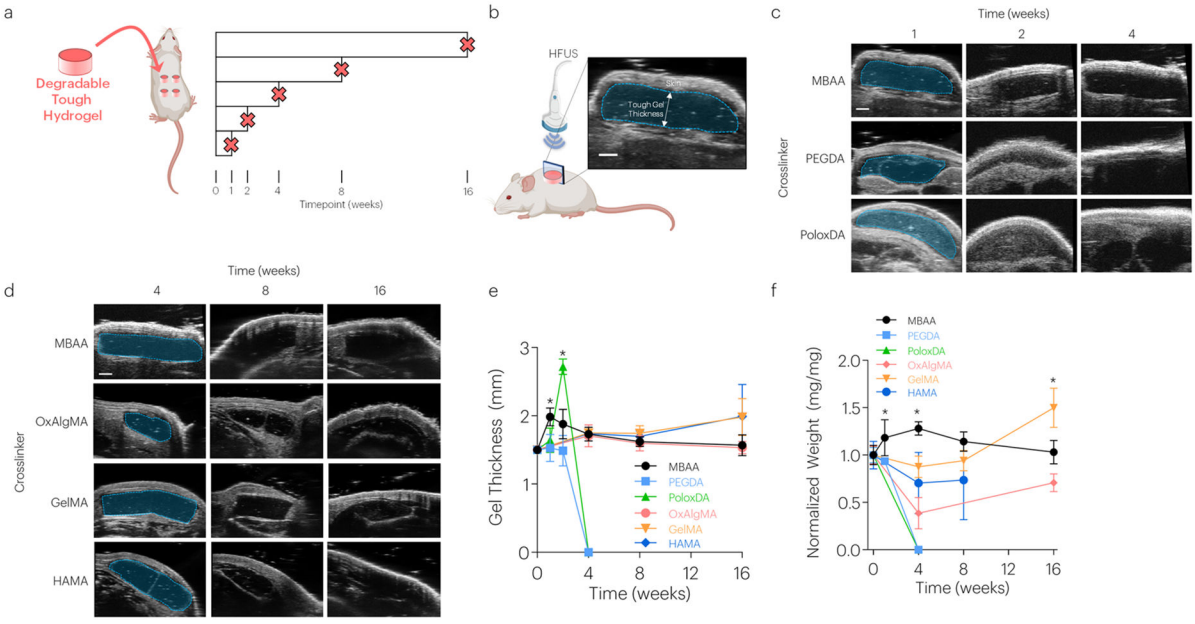

Figure 3: Tough Hydrogels with Degradable Covalent Network Demonstrate Tunable Degradation Profiles.

(**a**) Five different formulations of degradable tough hydrogels and non-degradable controls were implanted subcutaneously in mice and evaluated up to 16-weeks post implantation. (**b-e**) HFUS imaging evaluated changes in hydrogel thickness over time. **P*<0.01 between groups. Mean values are shown and error bars represent ± s.d. (n=3-4 samples/group), as analyzed by a one-way ANOVA with post hoc t-tests with Bonferroni correction. Scale bar = 1mm. (**f**) The effect of crosslinker type on TA dry weight post implantation. **P*<0.01 between groups. Mean values are shown and error bars represent ± s.d. (n=3-4 samples/group), as analyzed by a one-way ANOVA with post hoc t-tests with Bonferroni correction. Graphics generated in part with BioRender.

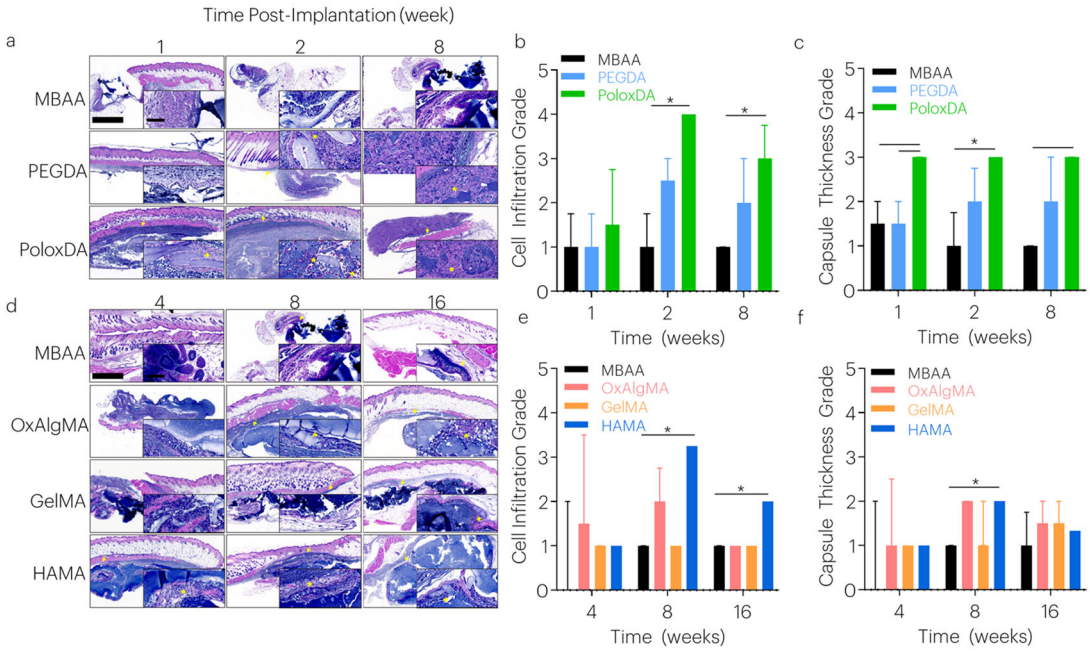

Figure 4: Tough Hydrogels with Degradable Covalent Network Demonstrate Biocompatibility.

Tissue histology samples were collected over time. (**a-c**) In fast degrading gels, cell infiltration and capsule thickness were evaluated after 1, 2, and 8 weeks. **P*<0.025 between groups. Median values are shown, and error bars represent IQR. (n=3-4 samples/group), as analyzed by a Scheirer-Ray-Hare test (nonparametric 2-way ANOVA) with Dunn's tests for multiple comparisons. Histological images are sagittal sections of tough hydrogel, surrounding soft tissue, and skin tissues stained with hematoxylin and eosin. Larger image scale bar: 1000μm. Inset scale bar: 100μm. The tough hydrogel stains dark blue with the basic hematoxylin; (blue) nuclei of leukocytes clustered at the periphery of the gel are also dark blue. Surrounding tissue, fibrous capsule, and subcutaneous muscle appear red with the acidic eosin component of the stain. Arrows indicate capsule. Asterisks indicate cell infiltration. (**d-f**) In slow degrading gels, cell infiltration and capsule thickness were evaluated after 4, 8, and 16 weeks. **P*<0.017 between groups. Median values are shown and error bars represent IQR. (n=3-4 samples/group), as analyzed by a Scheirer-Ray-Hare test (nonparametric 2-way ANOVA) with Dunn's tests for multiple comparisons. Histological images are sagittal sections of tough hydrogel, surrounding soft tissue, and skin tissues. Larger image scale bar: 1000μm. Inset scale bar: 100μm. The tough hydrogel stains dark blue with the basic hematoxylin; (blue) nuclei of leukocytes clustered at the periphery of the gel are also dark blue. Surrounding tissue, fibrous capsule, and subcutaneous muscle appear red with the acidic eosin component of the stain. Arrows indicate capsule. Asterisks indicate cell infiltration.

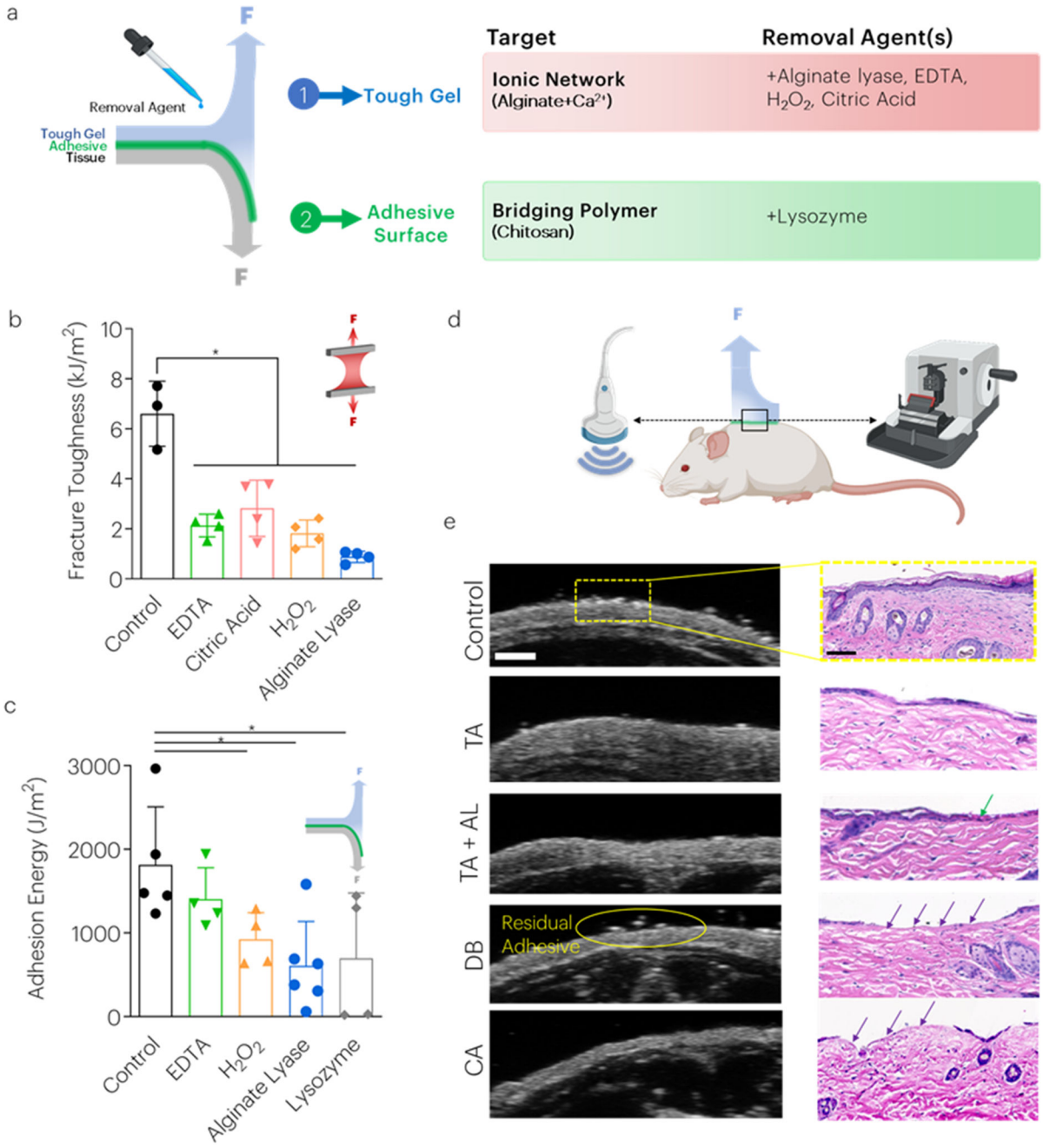

Figure 5: Removal agent treatments decrease tough adhesive toughness and adhesion energy on skin surfaces.

(**a**) Several strategies were tested to reduce the material properties and adhesion strength of the tough adhesives including the use of chemicals to chelate calcium ions from alginate and reduce molecular weight (**b**) Treatment with all chemicals decreased mechanical toughness. **P*<0.01 between groups. Mean values are shown and error bars represent ± s.d. (n=3-6 samples/group), as analyzed by a one-way ANOVA with post hoc t-tests with Bonferroni correction. (**c**) The adhesion energy following placement on porcine skin tissue was measured as a function of various treatments. **P*<0.01 between groups. Mean values

are shown and error bars represent ± s.d. (n=3-6 samples/group), as analyzed by a one-way ANOVA with post hoc t-tests with Bonferroni correction. (**d**) Following euthanasia, mouse skin was assessed using high frequency ultrasound and histology. (**e**) Control skin, and skin following removal of the TA (both without [TA] and with alginate lyase [TA+AL]), Dermabond [DB], and cyanoacrylate [CA] as assessed using high frequency ultrasound (left) and histology (right). Green arrows inside chitosan. Purple arrows indicate removal of the epidermis. Scale bar (HFUS) = 1mm. Scale bar (histology) = 100um. Graphics generated in part with BioRender.